

## Critical exponents of the three-dimensional diluted Ising model

H. G. Ballesteros,<sup>\*</sup> L. A. Fernández,<sup>†</sup> V. Martín-Mayor,<sup>‡</sup> and A. Muñoz Sudupe<sup>§</sup>  
*Departamento de Física Teórica I, Universidad Complutense de Madrid, 28040 Madrid, Spain*

G. Parisi<sup>\*\*</sup> and J. J. Ruiz-Lorenzo<sup>††</sup>  
*Dipartimento di Fisica and INFN, Università di Roma I, La Sapienza, P. A. Moro 2, 00185 Roma, Italy*  
 (Received 26 February 1998; revised manuscript received 6 April 1998)

We study the phase diagram of the site-diluted Ising model in a wide dilution range, through Monte Carlo simulations and finite-size scaling techniques. Our results for the critical exponents and universal cumulants turn out to be dilution independent, but only after a proper infinite volume extrapolation, taking into account the leading corrections-to-scaling terms. [S0163-1829(98)00429-9]

### I. INTRODUCTION

The magnetic phase diagram and critical properties of many magnetic materials can be described by means of the Heisenberg Hamiltonian:

$$H = \sum_{i,j,\alpha,\beta} J_{\alpha\beta}^{ij} S_i^\alpha S_j^\beta, \quad (1)$$

where  $S_i^\alpha$  is a spin operator. We use latin indices for lattice sites and greek ones for the spin components.  $J_{\alpha\beta}^{ij}$  is an usually short-ranged coupling matrix. One can understand Eq. (1) on the basis of the exchange interaction between the electrons of the external shells of the atoms. In principle, this interaction is O(3) symmetric. Nonetheless if one puts the atoms on a crystalline lattice, the material tends to magnetize in the so-called axes or planes of easy magnetization given by the symmetry of the crystal, thus breaking the O(3) symmetry.

A typical example is given by the uniaxial crystals, as the hexagonal lattices, where the magnetization can choose as subspace of easy magnetization the  $c$  axis or its orthogonal plane. In the first case the system is well described assuming that the magnetic momenta point in the  $c$  direction and it should be described by the Ising model. In the second one, the material should be studied by means of the XY model. One can use the form of Eq. (1) for these models, with an appropriate choice of the  $J$  matrix.

However no pure material exists in nature, so then it is mandatory to consider the effects of nonmagnetic impurities. The simplest way to do so is by considering a modified version of Eq. (1)

$$H = \sum_{i,j,\alpha,\beta} J_{\alpha\beta}^{ij} \epsilon_i \epsilon_j S_i^\alpha S_j^\beta, \quad (2)$$

where the  $\epsilon$ 's are quenched, uncorrelated random variables, chosen to be 1 with probability  $p$  (the spin concentration), or 0 with probability  $1-p$  (the impurity concentration, or spin dilution). The rationale for the quenched approximation is that usual relaxation times for the nonmagnetic impurities are much longer than the corresponding ones for spin dynamics. For nonfrustrated systems, the phase diagram of Eq.

(2) in the temperature-dilution plane consists of a magnetically disordered (paramagnetic) region at high temperature, separated from an ordered (ferromagnetic) region at lower temperatures (see Fig. 1). The dilution-dependent critical temperature  $T_c(p)$  obviously equals the pure model value at  $p=1$ . It lowers for larger dilution values, until the extreme case  $T_c(p_c)=0$  at the site percolation threshold for the concentration of the magnetic atoms.

Not many general results have been obtained for the Hamiltonian (2). The most popular one is doubtless the *Harris criterion*.<sup>1</sup> It states that the critical behavior of Eq. (2) will be the same as for Eq. (1) if the specific-heat critical exponent  $\alpha$  is negative, while a new universality class will appear if  $\alpha > 0$ . In the latter case it is possible to show<sup>2</sup> that  $\alpha$  for the diluted model is negative. The only model between the generic ones for magnetism (Ising, XY, Heisenberg) displaying  $\alpha > 0$  in three dimensions, is the Ising model.

There are other physical contexts in which the Hamiltonian (2) has been studied. For instance, its four-dimensional Ising version has been recently investigated (see Ref. 3 and references therein) in connection with the puzzling problem of finding nonasymptotically free interacting theories in four dimensions. The two-dimensional model is

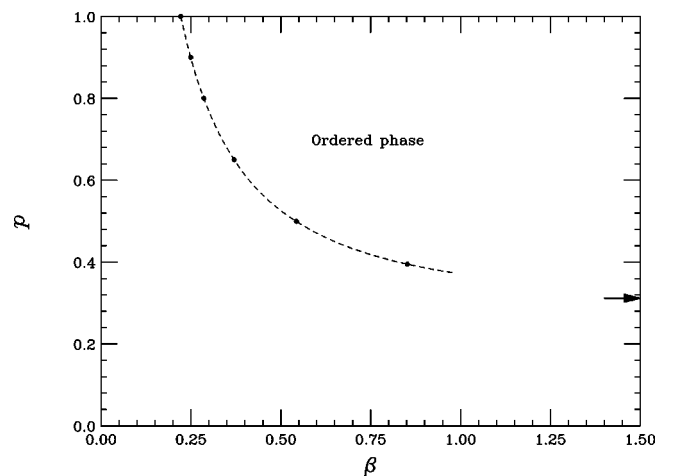


FIG. 1. Phase diagram of the model (3), in the inverse temperature-dilution plane. The dots correspond to the simulated points, while the arrow signals the percolation limit ( $\beta=\infty$ ).

TABLE I. Critical exponents for the diluted Ising model obtained from analytical calculations, and experimental measures. For comparison we also show the values for the pure Ising model.

	Ref.	$\nu$	$\gamma$	$\beta$	$\omega$
Analytical	9	0.697			0.416
	10	0.678	1.33	0.349	
	11	0.671	1.32	0.348	
	Ising (Ref. 12)	0.6300(15)	1.241(2)	0.3250(15)	0.78(2)
Experimental	23			0.36	
	24	$> 2/3$	1.44(6)		
	26			0.385(25)	
	25			0.350(9)	
	28	0.70(2)	1.37(4)		
	29	0.69(1)	1.31(3)		

also interesting as a playground for exactly solvable field theories, and has also been considered (see Refs. 4–8, and references therein).

As already stated, the materials displaying Ising-like behavior in very pure samples should behave differently when the impurities concentration increases. In fact, according to Harris, an infinitesimal impurity concentration should be enough to spoil the Ising behavior. However this will happen in very narrow intervals of temperature, which may be experimentally unreachable.

The Hamiltonian (2) can be studied in the low dilution regime by means of analytical perturbative renormalization-group methods.<sup>9–11</sup> They find a new fixed-point, thus implying that the critical exponents along the  $T_c(p)$  line are dilution independent and different from their pure Ising values. Their results are summarized in Table I. Unfortunately, the error estimations for this kind of calculations is very difficult.

The study of the Hamiltonian (2) beyond the low disorder regime, is restricted to the Monte Carlo (MC) method. Many simulations have been performed in the last 17 years.<sup>13–18</sup> The first study, on small lattices<sup>13</sup> was compatible with the new fixed-point scenario. However further simulations<sup>14</sup> found results rather suggesting a continuously varying value of the critical exponents along the critical line. A Monte Carlo renormalization-group study<sup>16</sup> found a value for the  $\nu$  exponent consistent with the perturbative one at  $p=0.8$ . However, for  $p=0.9$  their results did not differ from the pure Ising model, while for  $p<0.8$  they could not find meaningful results. More recent simulations<sup>15</sup> suggested a single fixed-point scenario with  $\nu=0.77(4)$ , confirmed in Ref. 17 where  $\nu=0.78(1)$  was found at  $p=0.4$ . This puzzle of mutually contradicting results started to make sense in Ref. 18, where the crucial observation that the exponents measured in a finite lattice are transitory was made. Unfortunately the statistical errors at large dilution did not allow for a definite conclusion.

Recently a MC work on this model has appeared.<sup>19</sup> They obtain  $\nu=0.682(2)$  at  $p=0.8$  but a markedly different result,  $\nu=0.717(8)$ , at  $p=0.6$ .

In this paper we present sound numerical evidence for a random fixed-point dominant along the whole critical line. This is achieved by means of a finite-size scaling (FSS) analysis, in a wide dilution range [ $0.4 \leq p \leq 0.9$ , the percola-

tion threshold being at  $p_c \approx 0.31$  (Ref. 20)]. The investigation of very diluted samples is made possible by a  $p$ -reweighting method, which allows us to extrapolate the simulation results obtained at  $p$  to a close  $p'$  value.<sup>3,6,21</sup> A careful consideration of the scaling corrections is needed, in order to get the right value in the infinite volume limit. In this system, the first corrections-to-scaling exponent,  $\omega$ , is very small ( $\omega \approx 0.4$ , see Ref. 9). Thus, the confusing results in previous MC studies can be understood as an unusually large contribution of the scaling corrections. After a proper consideration of this problem, we find dilution-independent critical exponents in quantitative agreement with perturbative calculations.

Another theoretical problem of interest is the absence of *self-averaging* at the critical point. This means that the disorder-realization variance of quantities such as the magnetic susceptibility or the specific heat, at the critical point, is a fixed, nonzero fraction of their mean values even in the thermodynamical limit. It has been argued<sup>22</sup> that this fixed fraction is an universal number. In Ref. 3, this fraction for the susceptibility is calculated analytically and numerically in four dimensions. In this work, we numerically calculate this ratio, along the critical line  $T_c(p)$ . After the compulsory infinite volume extrapolation, a universal, dilution-independent result is found. A very recent simulation<sup>19</sup> has questioned the universality of these ratios. However, these authors do not perform any infinite volume extrapolation, thus their conclusions are necessarily not definitive.

The experimental study is still not completed (see Table I). For instance, indications of the expected new universality class were obtained<sup>23,24</sup> in the Ising antiferromagnet  $\text{Fe}_{1-x}\text{Zn}_x\text{F}_2$ , studied in the reduced temperature range  $10^{-3} \leq t \leq 10^{-1}$ . Also in Ref. 24, a cusplike behavior of the specific heat was found, so no divergence was expected. This yields  $\nu \geq 2/3$  through standard hyperscaling relations. Mössbauer measurements in  $\text{Fe}_{0.9}\text{Zn}_{0.1}\text{F}_2$  gave similar results.<sup>25</sup> A compatible value for the exponent  $\beta$  was obtained for a dysprosium aluminum garnet doped with yttrium at a 5% dilution.<sup>26</sup> The results regarding the  $\beta$  exponent have been questioned in Ref. 27 where  $\text{Mn}_{0.5}\text{Zn}_{0.5}\text{F}_2$  was studied by synchrotron magnetic x-ray scattering. These authors conclude that the experimental errors to date are too big to distinguish between the pure Ising and the diluted  $\beta$  values.

Maybe the strongest evidence found for a new universality class regards exponents  $\gamma$  and  $\nu$ . The best measures have been reported in Refs. 28,29; they were obtained by means of neutron scattering in  $\text{Mn}_{1-x}\text{Zn}_x\text{F}_2$  and  $\text{Fe}_x\text{Zn}_{1-x}\text{F}_2$ , respectively.

The layout of the paper is as follows. In Sec. II we define the model and the observables to be measured in the numerical simulation. In Sec. III we provide the necessary technical details about the MC methods. Section IV is devoted to finite-size scaling techniques. After that, in Sec. V, we present our numerical results and discuss the need for an infinite-volume extrapolation. This is considered in Sec. VI. We present our conclusions in Sec. VII.

## II. THE MODEL

We have considered the site-diluted Ising model on the single-cubic lattice, with nearest-neighbor interaction. We will work in a lattice of linear size  $L$ , with periodic boundary conditions. The Hamiltonian is

$$H = -\beta \sum_{\langle i,j \rangle} \epsilon_i \epsilon_j \sigma_i \sigma_j, \quad (3)$$

where  $\sigma$  are the usual  $Z_2$  spin variables. The  $\epsilon$ 's are the quenched random variables introduced in Eq. (2). We shall refer to an actual  $\{\epsilon_i\}$  configuration as a *sample*. We study the so-called quenched disorder: that is, for every observable it is understood that we *first* calculate the average on the  $\{\sigma_i\}$  variables with the Boltzmann weight given by  $\exp(-H)$ , the results on the different samples being *later* averaged.

To avoid confusion, we will denote the Ising average with brackets, while the subsequent sample average will be overlined. The observables will be denoted with calligraphic letters, i.e.,  $\mathcal{O}$ , and with italics the double average  $O = \langle \mathcal{O} \rangle$ . The total nearest-neighbor energy is defined as

$$\mathcal{E} = \sum_{\langle i,j \rangle} \epsilon_i \sigma_i \epsilon_j \sigma_j. \quad (4)$$

The energy is extensively used for extrapolating the results obtained for an observable,  $O$ , at coupling  $\beta$  to a nearby  $\beta'$  coupling<sup>30</sup> and for calculating  $\beta$  derivatives through its connected correlation. For instance, one can define the specific heat as

$$C = \partial_\beta \overline{\langle \mathcal{E} \rangle} = \frac{1}{V} (\overline{\langle \mathcal{E}^2 \rangle} - \langle \mathcal{E} \rangle^2), \quad (5)$$

$V$  being the total number of sites in the lattice,  $L^3$ .

The normalized magnetization is

$$\mathcal{M} = \frac{1}{V} \sum_i \epsilon_i \sigma_i. \quad (6)$$

In terms of the magnetization we can give a convenient definition of the susceptibility as

$$\chi = V \overline{\langle \mathcal{M}^2 \rangle}, \quad (7)$$

its Binder parameter being

$$g_4 = \frac{3}{2} - \frac{1}{2} \frac{\overline{\langle \mathcal{M}^4 \rangle}}{\overline{\langle \mathcal{M}^2 \rangle}^2}. \quad (8)$$

Another kind of cumulant, meaningless for the pure system, can be defined as

$$g_2 = \frac{\overline{\langle \mathcal{M}^2 \rangle^2} - \langle \mathcal{M}^2 \rangle^2}{\overline{\langle \mathcal{M}^2 \rangle}^2}. \quad (9)$$

This quantity would be zero in the thermodynamical limit if self-averaging is to be found. A very useful definition of the correlation length in a finite lattice, reads<sup>31</sup>

$$\xi = \left( \frac{\chi/F - 1}{4 \sin^2(\pi/L)} \right)^{1/2}, \quad (10)$$

where  $F$  is defined in terms of the Fourier transform of the magnetization

$$\mathcal{G}(\mathbf{k}) = \frac{1}{V} \sum_{\mathbf{r}} e^{i\mathbf{k} \cdot \mathbf{r}} \epsilon_{\mathbf{r}} \sigma_{\mathbf{r}}, \quad (11)$$

as

$$F = \frac{V}{3} \langle |\mathcal{G}(2\pi/L, 0, 0)|^2 + \text{permutations} \rangle. \quad (12)$$

This definition is very well behaved for the FSS method we employ.<sup>32</sup>

## III. THE MONTE CARLO UPDATE

The method of choice for an Ising model simulation is a cluster method. The most efficient variety for the pure model is the Wolff's single-cluster (SC) update.<sup>33</sup> However, in diluted systems one can find groups of spins almost completely surrounded by holes that are scarcely changed with a SC method. Thus we have carefully studied the problem of the thermalization for each value of the dilution.

We have found two different regimes. For small dilution ( $p \geq 0.65$ ), the mean size of the groups is small and can be appropriately thermalized by adding a Metropolis update. For larger dilutions ( $p \leq 0.5$ ), using the same update methods, the integrated autocorrelation times do not show a significant increase, and a plot of the measures against the MC time does not show any significant drift. However, we observe deviations coming from hot and cold starts. This failure is due to the presence of intermediate-sized groups of nearly isolated spins that neither Metropolis nor SC can efficiently thermalize. In this cases we have found that the addition of a Swendsen-Wang (SW) cluster update<sup>34</sup> is enough to provide a fast thermalization.

Thus we have constructed our elementary MC step (EMCS) as 250 SC flips complemented with a Metropolis step for  $p \geq 0.65$  and a SW sweep every 200 SC flips for the other dilutions. We discard 100 EMCS for equilibration, then measuring after every EMCS. The integrated autocorrelation times for all observables are very small: near 1 EMCS in the largest lattice.

A disordered model simulation gets characterized by two parameters, the number of samples generated ( $N_S$ ) and the

number of independent measures taken in each sample ( $N_I$ ). Previous works (for instance Refs. 16–18) have chosen the  $N_I \gg N_S$  regime. However (see Ref. 3), the optimal regime is

$$N_I \sim \left( \frac{\sigma_I}{\sigma_S} \right)^2, \quad (13)$$

where  $\sigma_I$  is the mean variance *in a sample* of the observable under consideration, while  $\sigma_S$  is the variance *between different samples*. Moreover, the nonvanishing value of  $g_2$  shows that the susceptibility is not a self-averaging quantity, thus making very dangerous the small  $N_S$  regime. In this work we have fixed  $N_I = 200$  and  $N_S = 20\,000$ . For  $p = 0.9$  we performed  $N_S = 10\,000$ .

In addition to the usual  $\beta$  extrapolation,<sup>30</sup> in some cases it is useful to perform a  $p$  extrapolation. It can be done as we know the precise distribution of the densities of the actual configurations (binomial distribution). Details of the method can be found in Ref. 3 for the same model in four dimensions.

We remark that when computing  $\beta$  derivatives of observables,  $\partial_\beta \langle \mathcal{O} \rangle = \langle \mathcal{O} \mathcal{E} \rangle - \langle \mathcal{O} \rangle \langle \mathcal{E} \rangle$ , or the  $\beta$  extrapolation,  $\langle \mathcal{O} \rangle (\beta + \Delta\beta) = \langle \mathcal{O} e^{\Delta\beta \mathcal{E}} \rangle / \langle e^{\Delta\beta \mathcal{E}} \rangle$ , we suffer a bias that decreases as  $1/N_I$ , if the measures used for computing the different mean values are not statistically independent. This is negligible in usual MC simulations where the statistical error is larger (of order  $1/\sqrt{N_I}$ ). However, when averaging in many different samples, the statistical error can become too small to ignore the bias. Fortunately, there are several methods to eliminate it. For instance, we use subsets of measures to parameterize the bias as a function of  $N_I$  and then to extrapolate  $N_I \rightarrow \infty$ . Further details can be found in Ref. 3 where the method was applied in the four-dimensional diluted Ising model.

#### IV. FINITE-SIZE SCALING METHODS

A very efficient way of measuring critical exponents<sup>32</sup> follows from this form of the FSS ansatz:

$$O(L, \beta, p) = L^{x_O/\nu} [F_O(\xi(L, \beta, p)/L) + O(L^{-\omega})], \quad (14)$$

where a critical behavior  $t^{-x_O}$  is expected for the operator  $O$ , and  $F_O$  is a (smooth) scaling function. From a renormalization-group point of view,  $\omega$  is the eigenvalue corresponding to the leading irrelevant operator. It is very important that, in the above equation, only quantities measurable on a finite lattice appear. Notice that terms of order  $\xi_{L=\infty}^{-\omega}$  are dropped from Eq. (14), so we assume that we are deep within the scaling region.

To eliminate the unknown scaling function, we measure the quotient

$$Q_O = O(sL, \beta, p) / O(L, \beta, p), \quad (15)$$

at the coupling value for which the correlation length in units of the lattice size is the same for both lattices. So we get

$$Q_O|_{Q_\xi=s} = s^{x_O/\nu} + O(L^{-\omega}). \quad (16)$$

Given the strong statistical correlation between  $Q_O$  and  $Q_\xi$ , the above quotient can be obtained with great accuracy (in

fact, in our opinion, this is the best available method to measure the usually tiny three-dimensional  $\eta$  exponents<sup>32</sup>).

In many cases (high precision computations or small lattices), it is useful to parametrize the leading corrections-to-scaling, thus we need to consider in the analysis a behavior like

$$Q_O|_{Q_\xi=s} = s^{x_O/\nu} + A_p^O L^{-\omega} + \dots \quad (17)$$

Here the dots stand for higher-order corrections, while  $A_p^O$  is a dilution-dependent slope.

The most convenient observables to measure the two independent critical exponents,  $\eta$  and  $\nu$ , are found to be

$$\partial_\beta \xi \rightarrow x = \nu + 1,$$

$$\chi \rightarrow x = \nu(2 - \eta).$$

#### V. NUMERICAL RESULTS

The phase diagram of the model (3) is shown in Fig. 1. In this work we have simulated lattices  $L = 8, 16, 32, 64$ , and  $128$ , at dilutions  $p = 0.9, 0.8, 0.65, 0.5$ , and  $0.4$ . Our procedure has been the following. For  $p = 0.9, 0.8, 0.65$ , we have chosen a  $\beta$  coupling value where the relation

$$\frac{\xi(L, \beta, p)}{L} = \frac{\xi(2L, \beta, p)}{2L} \quad (18)$$

approximately holds. Then, we have relied on standard reweighting methods, which allow us to extrapolate the simulation results at coupling  $\beta$  to a close  $\beta'$ , to precisely fulfill the matching condition (18). For very diluted systems, the transition line is almost horizontal (see Fig. 1) thus it is more convenient to use a  $p$ -reweighting method to extrapolate the simulation results to a nearby  $p'$  value (see Refs. 3, 6, 21). Therefore, we have first located the  $\beta$  values for which Eq. (18) holds at  $p = 0.4, 0.5$ , then we have fixed this  $\beta$  value, and changed  $p$  later on. In this way, the true critical dilutions for fixed  $\beta$ ,  $p_c(\beta)$ , differ from  $0.4$  and  $0.5$  (in less than a 2%). Nevertheless, we shall keep referring to them as  $p = 0.4, 0.5$  in tables and graphics, for the sake of clarity.

In Table II we present the results for exponents  $\nu$  and  $\eta$  and cumulants  $g_4$  and  $g_2$ , using Eq. (16) (neglecting scaling corrections). Beware that consecutive data in the table are anticorrelated [the results of lattice  $L$  are used once in the numerator and another time in the denominator in Eq. (16)]. For the error computation we have used a jack-knife method with 50 bins, ensuring a 10% of uncertainty in the error bars. Thus, we display two digits in these bars if the first one is smaller than 5.

Notice that the exponent  $\eta$  and the cumulant  $g_4$  are, before any infinite volume extrapolation, quite dilution independent. This can be understood because they show a very mild evolution with the lattice size. On the contrary, exponent  $\nu$  and cumulant  $g_2$  show a larger dependence on the lattice size and so, an infinite volume extrapolation is needed before one can extract definite conclusions. Nevertheless, one can already guess from the table that  $\nu$  is surely different from the pure Ising value and the  $g_2$  cumulant is different from zero (there is not self-averaging). The latter was also

TABLE II. Critical quantities obtained from pairs  $(L, 2L)$  using Eq. (16) for all the dilutions simulated.

	$L$	$p=0.9$	$p=0.8$	$p=0.65$	$p=0.5$	$p=0.4$
$\eta$	8	0.0171(7)	0.0219(7)	0.0284(10)	0.0296(24)	0.0322(29)
	16	0.0277(7)	0.0308(7)	0.0330(8)	0.0345(19)	0.0297(16)
	32	0.0320(9)	0.0335(8)	0.0329(9)	0.0313(11)	0.0315(17)
	64	0.0349(9)	0.0346(8)	0.0335(8)	0.0329(14)	0.0326(13)
$\nu$	8	0.6663(14)	0.6877(11)	0.7172(16)	0.7447(24)	0.7718(32)
	16	0.6643(14)	0.6849(12)	0.7107(18)	0.7328(22)	0.7534(32)
	32	0.6631(15)	0.6836(12)	0.7048(20)	0.7189(24)	0.7382(27)
	64	0.6644(15)	0.6864(14)	0.6996(20)	0.7118(21)	0.7182(26)
$g_2$	8	0.0832(10)	0.1546(16)	0.2310(25)	0.2784(24)	0.3043(24)
	16	0.0861(12)	0.1500(14)	0.2077(15)	0.2371(20)	0.2551(22)
	32	0.0918(13)	0.1474(17)	0.1920(20)	0.2138(22)	0.2296(25)
	64	0.0974(17)	0.1477(12)	0.1842(19)	0.1994(21)	0.2106(16)
$g_4$	8	0.7049(14)	0.6900(17)	0.6814(23)	0.6900(20)	0.6989(20)
	16	0.6926(17)	0.6818(15)	0.6809(16)	0.6871(18)	0.6958(21)
	32	0.6876(19)	0.6819(16)	0.6832(20)	0.6879(17)	0.6889(20)
	64	0.6821(16)	0.6771(18)	0.6780(17)	0.6825(19)	0.6857(22)

observed in the same model in four dimensions,<sup>3</sup> where we found mean-field results plus logarithmic corrections.

Another quantity of interest is the specific heat. As stated in the introduction,  $\alpha$  is negative and no divergences are expected. This is a quite difficult behavior to study, because FSS investigations in other models displaying  $\alpha < 0$ , show that the specific heat at the critical point is a growing, though bounded, quantity.<sup>32</sup> For this reason we choose to study

$$\Delta C(L) = [C(2L) - C(L)]_{Q_{\xi}^2=2}.$$

It diverges if  $\alpha > 0$ , tends to zero if  $\alpha < 0$  and goes to a constant value if the specific heat diverges logarithmically ( $\alpha = 0$ ). In addition, the usually large background term of the specific-heat disappears. It will be convenient to recall that by deriving the FSS ansatz from the renormalization group,<sup>35</sup> one finds a behavior for the specific heat as  $L^{2y_T-d}$  (where  $y_T = 1/\nu$ ). Therefore one should expect the fulfillment of hyperscaling relations for the transient exponents,  $\alpha(L)$

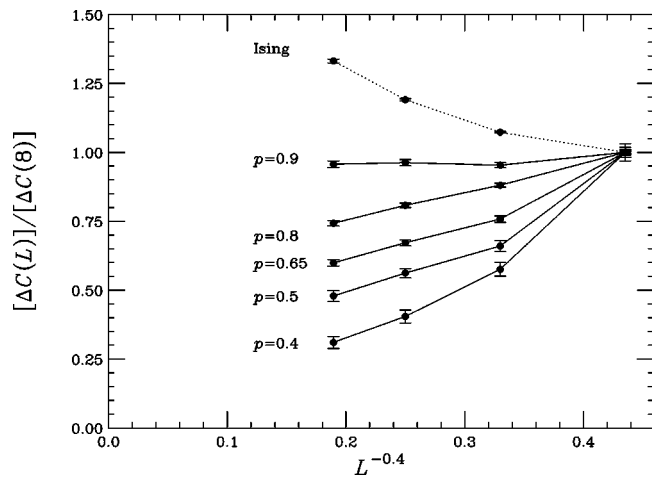


FIG. 2. Normalized specific-heat difference at the point where  $Q_{\xi}^2=2$ . The  $\omega \approx 0.4$  value used in the plot is obtained in Ref. 9.

and  $\nu(L)$ . In Fig. 2 we plot the  $\Delta C(L)$  values obtained. As a contrast we also plot the corresponding values for the pure Ising model which grow, as they should (the data are taken from Ref. 36). We find a decreasing value of  $\Delta C(L)$  for  $p \leq 0.8$ , as expected. Notice that the (transient)  $\nu \approx 2/3$  found for  $p=0.9$  in Table II, implies  $\alpha=0$  through hyperscaling relations. This is very nicely shown in the plot, where a constant value of  $\Delta C(L, p=0.9)$  is seen. Plotting  $\Delta C(L)$  against  $L^{\alpha/\nu}$  would be useless, because the scaling corrections go approximately as  $L^{-0.4}$ , that is, their lattice size evolution is much faster than that of the asymptotic term.

## VI. INFINITE VOLUME EXTRAPOLATION

As shown in the previous section, with our statistical accuracy the values for the critical exponents are seen to depend on the lattice size, so an infinite volume extrapolation is

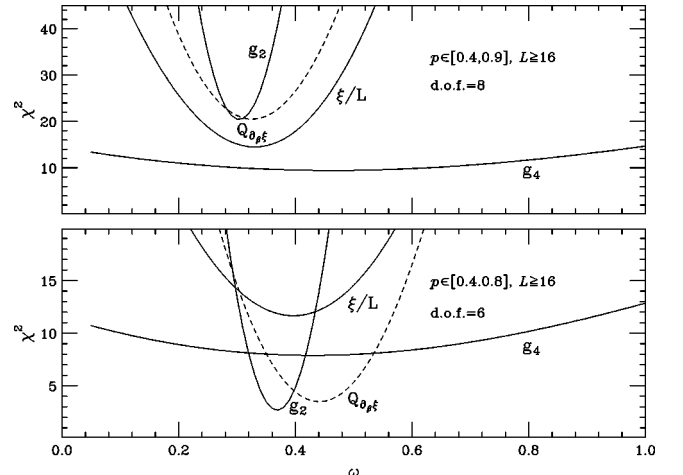


FIG. 3. Minimum of  $\chi^2$  as a function of  $\omega$ , for the fits of Eq. (19). We also plot with a dashed line the corresponding quantity for the  $Q_{\partial\rho\xi}$  fit.

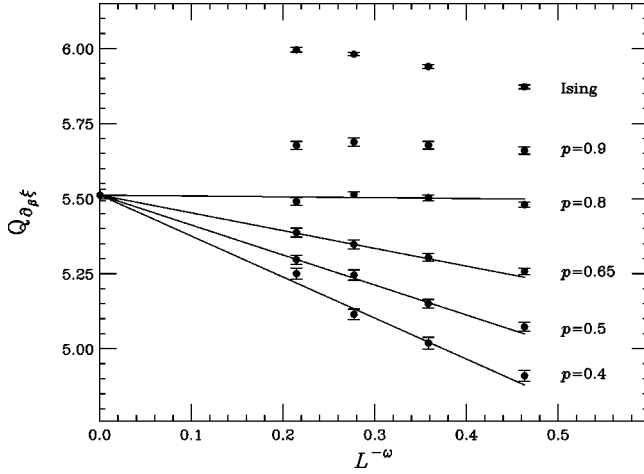


FIG. 4.  $Q_{\partial_{\beta\xi}} = 2^{1+1/\nu}$  for the different dilutions. The solid lines correspond to a fit enforced to yield the same infinite volume extrapolation for  $p \leq 0.8$ . The smallest lattice in the fit is  $L=8$  and we use  $\omega=0.37$ . The Ising data have been taken from Ref. 36.

required [see Eq. (17)]. However, one has to decide when the dots in Eq. (17) can be neglected. Our criterium will be the following. We perform the fit for lattice sizes not smaller than a given  $L_{\min}$ . If the fit quality is reasonable (i.e., a not too large  $\chi^2/\text{degree of freedom}$  (dof) calculated with the full covariance matrix), we repeat it for lattices not smaller than  $2L_{\min}$ . If this last fit is also reasonable and *the extrapolated values are compatible in both fits*, we keep the central value from the  $L_{\min}$  fit, but quote error bars from the  $2L_{\min}$  one.

Therefore the needed estimate for  $\omega$ , will be obtained from the lattice size evolution of the scaling functions:

$$\begin{aligned} \left. \frac{\xi}{L} \right|_{Q_{\xi}=2} &= \left( \frac{\xi}{L} \right)^{\infty} + A_p^{\xi} L^{-\omega} + \dots, \\ g_4 \Big|_{Q_{\xi}=2} &= g_4^{\infty} + A_p^{g_4} L^{-\omega} + \dots, \\ g_2 \Big|_{Q_{\xi}=2} &= g_2^{\infty} + A_p^{g_2} L^{-\omega} + \dots. \end{aligned} \quad (19)$$

Then we shall use this  $\omega$  value to extrapolate the critical exponents  $\nu$  and  $\eta$ . A reasonable value of  $\chi^2/\text{dof}$  in these fits will be a consistency condition. A technical point of interest is that the single universality-class scenario requires the infinite volume extrapolation for  $g^{\chi^2/\nu}$  to be dilution independent. Therefore, we can include data of different dilutions and lattice sizes in the fit.

In Fig. 3, we plot the minimum of  $\chi^2/\text{dof}$  in a fit to Eq. (19), as a function of  $\omega$ . Several points become clear. It is obvious that  $g_4$  is not useful at all in order to fix  $\omega$  (this is

TABLE III. Results of the infinite volume extrapolation of  $g_2$  and  $\xi/L$ , including data from  $L \geq L_{\min}$ , at  $p=0.4, 0.5, 0.65$ , and  $0.8$ .  $Q(\chi^2, \text{dof})$  is the probability of getting a larger  $\chi^2$  in the fit.

$L_{\min}$	$\chi^2/\text{dof}$	$Q$	$\omega$	$\xi/L$	$g_2$
8	46.2/21	0.0012	0.430(15)	0.5890(17)	0.1458(17)
16	15.0/13	0.31	0.37(2)	0.598(4)	0.145(3)
32	1.95/5	0.86	0.38(6)	0.587(7)	0.150(7)

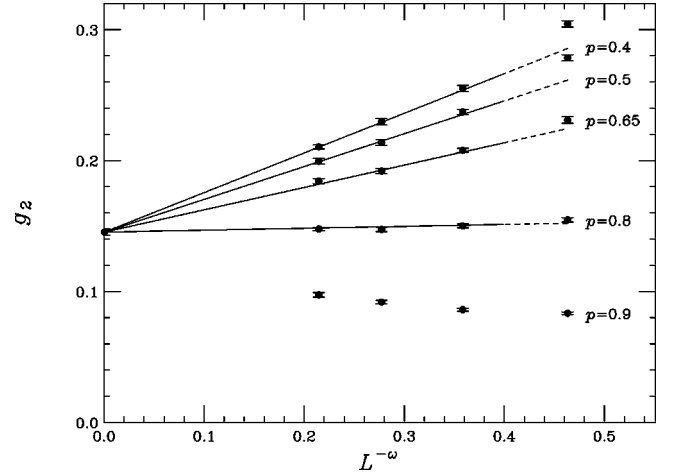


FIG. 5. Cumulant  $g_2$  as a function of  $L^{-\omega}$ . The solid lines correspond to a fit enforced to yield the same infinite volume extrapolation for  $p \leq 0.8$ . The smallest lattice in the fit is  $L=16$  and we use  $\omega=0.37$ .

not surprising as it shows almost no scaling corrections,  $A_p^{g_4} \approx 0$ ). We see that including the  $p=0.9$  data yields an untenable fit with  $L_{\min}=16$ . Moreover, when we study the extrapolation for  $Q_{\partial_{\beta\xi}} = 2^{1+1/\nu}$ , we find an awful result. This could have been anticipated from Fig. 2, where a clearly nonasymptotic value for the specific heat at  $p=0.9$  is seen. On the contrary, when discarding the  $p=0.9$  data, reasonable fits are obtained. Thus, we conclude that the  $p=0.9$  system is still crossing over from the pure Ising fixed point to the diluted one, even for lattices as large as  $L=128$ . Finally, it is evident from the plot that the determination of  $\omega$  can be greatly improved by means of a *joint fit* of the  $g_2$  and  $\xi/L$  scaling functions. The results for this fit are shown in Table III. According to our, conservative, dots-neglecting criterium, we find

$$\omega = 0.37(6). \quad (20)$$

Notice that the value obtained in Ref. 9,  $\omega=0.42$  (without error estimation), using the scaling-field method for momentum-space RG equations, is compatible with ours.

In Table IV we present the infinite volume extrapolation

TABLE IV. Infinite volume extrapolation and fit qualities for the critical exponents, including data from  $L \geq L_{\min}$ , at  $p=0.4, 0.5, 0.65$ , and  $0.8$  using Eq. (17). The second error is due to the indetermination in  $\omega=0.37(6)$ .

	$L_{\min}$	Extrapolation	$\chi^2/\text{dof}$	$Q$
$\nu$	8	0.6837(10)(29)	14.0/11	0.24
	16	0.6838(24)(33)	6.26/7	0.51
	32	0.687(6)(2)	4.14/3	0.25
$\eta$	8	0.0419(8)(20)	96.4/11	$< 10^{-15}$
	16	0.0374(12)(9)	8.92/7	0.26
	32	0.0374(36)(8)	0.18/3	0.98
$g_4$	8	0.6726(21)(25)	31.5/11	.0001
	16	0.6734(28)(21)	7.95/7	0.34
	32	0.665(7)(3)	1.08/3	0.78

TABLE V. Crossing points of scaling functions  $\xi/L$  and  $g_4$  for pairs  $L$  and  $2L$  for the different dilutions.

	$L$	$p=0.9$	$p=0.8$	$p=0.65$	$p=0.5$	$p=0.4$
$g_4$	8	0.249583(30)	0.286002(48)	0.37025(13)	0.49996(27)	0.39577(28)
	16	0.249340(15)	0.285765(18)	0.370185(36)	0.49949(6)	0.39512(8)
	32	0.2492901(13)	0.285758(7)	0.370208(16)	0.499485(30)	0.394895(33)
	64	0.2492924(15)	0.2857417(25)	0.3701649(48)	0.499409(11)	0.394840(13)
$\xi/L$	8	0.249299(26)	0.285690(49)	0.36961(10)	0.49814(17)	0.39302(19)
	16	0.249291(12)	0.285708(15)	0.369986(31)	0.49896(5)	0.39441(6)
	32	0.2492957(44)	0.285745(6)	0.370147(13)	0.499326(21)	0.394694(23)
	64	0.2492901(13)	0.2857394(23)	0.3701540(44)	0.499374(9)	0.394785(10)

for  $\nu$  and  $\eta$  critical exponents and the  $g_4$  cumulant. We see that  $L_{\min}=16$  fulfills our dots-neglecting criterium for  $g_4$  and  $\eta$ . For  $\nu$ ,  $L_{\min}=8$  is found to be enough. Our final values are

$$\begin{aligned}\nu &= 0.6837(24)(29), \\ \eta &= 0.0374(36)(9), \\ g_4 &= 0.673(7)(2),\end{aligned}\tag{21}$$

where the first error is statistical while the second is due to the uncertainty in  $\omega$ . From Eq. (21) we obtain

$$\begin{aligned}\alpha &= -0.051(7)(9), \\ \beta &= 0.3546(18)(10), \\ \gamma &= 1.342(5)(5).\end{aligned}\tag{22}$$

For the computation of the statistical error in  $\beta$  and  $\gamma$  we take into account that the statistical correlation between  $\nu$  and  $\eta$  has turned out to be negligible. The agreement with experimental measures of  $\nu$  and  $\gamma$  (see Table I) is very good.

In Fig. 4 we show  $Q_{\partial\beta\xi}$  as a function of  $\omega$  for all the dilutions. We also plot the corresponding values for the pure Ising model. The solid lines correspond to the joint fit for  $L_{\min}=8$  using the data from  $p\leq 0.8$ . Notice that the data are strongly anticorrelated, therefore the apparent  $\chi^2$  on the plot is larger than the real one, computed with the full covariance matrix. An analogous fit for  $g_2$  is shown in Fig. 5. We remark that the  $p=0.9$  data are pointing to a (maybe) too-low value. This is another signature of the crossover from the Ising fixed point ( $g_2=0$ ) to the diluted one.

It is interesting to compare the values for  $g_4$  and  $g_2$  with those obtained in four dimensions:<sup>3</sup>

$$\begin{aligned}g_4 &= 0.32455, \\ g_2 &= 0.31024.\end{aligned}$$

Finally, we can compute the infinite volume critical couplings by studying the crossing points of scaling functions (as  $\xi/L$  and  $g_4$ ) measured in lattices of sizes  $L$  and  $sL$ . Let  $\Delta\beta_c^L, \Delta p_c^L$  be the deviation of these crossing points from the infinite-volume critical couplings. The expected scaling behavior is<sup>37</sup>

$$\Delta\beta_c^L, \Delta p_c^L \propto \frac{1-s^{-\omega}}{s^{1/\nu}-1} L^{-\omega-1/\nu}.\tag{23}$$

In Table V we present the crossing points of  $\xi/L$  and  $g_4$  for the  $(L, 2L)$  pair for all the dilutions simulated. We find again that an infinite volume extrapolation is needed in order to extract the critical couplings.

Using Eq. (23) for  $s=2$  we perform a joint fit for both scaling functions  $g_4$  and  $\xi/L$ . For this fit we take  $\omega+1/\nu=1.83(6)$ . The final results for the different dilutions studied are shown in Table VI, where two values for  $L_{\min}$  are used. Let us remark that our critical couplings are compatible with the results in Ref. 18 [ $\beta_c^{p=0.8}=0.28578(4)$ ,  $\beta_c^{p=0.9}=0.24933(3)$ ]. But we definitely do not agree with the value  $\beta_c^{p=0.8}=0.2857609(4)$  quoted in Ref. 19. This is not surprising as in this work the corrections-to-scaling are not considered.

## VII. CONCLUSIONS

We have shown, beyond the low-disorder limit, that the diluted Ising model is in the basin of attraction of a single fixed point. Therefore, if randomness is to be modeled with Eq. (2), the critical exponents of an Ising system are not those of the pure Ising model, but those of the random fixed point (although this may be fairly hard to show in a very pure sample). To establish this result we have simulated in a very wide dilution range, finding a consistent picture *only after an infinite volume extrapolation*. The  $p=0.9$  data seem,

TABLE VI. Infinite volume critical couplings estimations for the studied dilutions. The first error bar corresponds to the statistical fit error, the second one (almost negligible) is due to the uncertainty in  $\omega+1/\nu$  exponent. For this table we use  $\omega+1/\nu=1.83(6)$ .

$L_{\min}$	$\chi^2/\text{dof}$	$p_c$	$\beta_c$
16	0.11/3	0.394816(11)(2)	0.852
32	0.04/1	0.394821(22)(7)	0.852
16	2.93/3	0.499413(9)(1)	0.543
32	0.78/1	0.499394(17)(4)	0.543
16	5.27/3	0.65	0.370166(5)(1)
32	1.53/1	0.65	0.370156(8)(0)
16	5.41/3	0.8	0.2857421(30)(0)
32	0.27/1	0.8	0.2857368(47)(5)
16	8.45/3	0.9	0.2492905(19)(0)
32	0.03/1	0.9	0.2492880(30)(5)

however, to be still crossing over from the pure Ising fixed point to the diluted one in lattices as large as  $L = 128$ .

We obtain the values of the critical exponents and universal cumulants eliminating the systematic errors coming from the leading corrections-to-scaling terms. The previous MC computations did not consider these terms and were not able to control the corresponding systematic effects. Incidentally, most of the computations have been carried out at  $p = 0.8$  as in this case the scaling corrections are very small, and the results in small lattices seem stable. However, even in this case the lack of an extrapolation produces an underestimation of the errors.

The (dilution-independent) critical exponents are shown to be in good agreement with the series estimates.<sup>9-11</sup> The corrections-to-scaling exponent  $\omega$  is measured with a 16% error and is found to be in quantitative agreement with the perturbative estimate.<sup>9</sup> The smallness of this exponent explains why this problem is so hard to attack numerically. In fact, the total computer time devoted to this work has been about five Intel Pentium-Pro years. As we had already shown

in four dimensions,<sup>3</sup> diluted Ising models are found not to be self-averaging at criticality in three dimensions (see Ref. 19 for an independent verification in three dimensions). This is proved by showing that the quotient between the sample variance of the susceptibility and its mean value tends in the thermodynamic limit to a nonzero constant independent of the dilution (it is a renormalization-group invariant). This quotient is measured with a 4% accuracy after the infinite volume extrapolation.

## ACKNOWLEDGMENTS

We are grateful to Dave Belanger for calling our attention to relevant experimental work. The computations have been carried out using the RTNN machines at Universidad de Zaragoza and Universidad Complutense de Madrid. We acknowledge CICyT for partial financial support (AEN97-1708 and AEN97-1693). J.J.R.L. is granted by EC HMC (ERBFMBICT950429).

\*Electronic address: hector@lattice.fis.ucm.es

†Electronic address: laf@lattice.fis.ucm.es

‡Electronic address: victor@lattice.fis.ucm.es

§Electronic address: sudupe@lattice.fis.ucm.es

\*\*Electronic address: giorgio.parisi@roma1.infn.es

††Electronic address: ruiz@chimera.roma1.infn.es

<sup>1</sup>A. B. Harris, J. Phys. C **7**, 1671 (1974).

<sup>2</sup>J. T. Chayes, L. Chayes, D. S. Fisher, and T. Spencer, Phys. Rev. Lett. **57**, 2999 (1986).

<sup>3</sup>H. G. Ballesteros, L. A. Fernández, V. Martín-Mayor, A. Muñoz Sudupe, G. Parisi, and J. J. Ruiz-Lorenzo, Nucl. Phys. B **512**[FS], 681 (1998).

<sup>4</sup>Vik. S. Dotsenko and Vl. S. Dotsenko, JETP Lett. **33**, 37 (1981); Adv. Phys. **32**, 129 (1983).

<sup>5</sup>J. Cardy J. Phys. A **29**, 1897 (1996).

<sup>6</sup>H. G. Ballesteros, L. A. Fernández, V. Martín-Mayor, A. Muñoz Sudupe, G. Parisi, and J. J. Ruiz-Lorenzo, J. Phys. A **30**, 8379 (1997).

<sup>7</sup>J. J. Ruiz-Lorenzo, J. Phys. A **30**, 485 (1997).

<sup>8</sup>F. D. A. Aarão Reis, S. L. A. de Queiroz, and R. R. dos Santos, Phys. Rev. B **56**, 6013 (1997).

<sup>9</sup>K. E. Newman and E. K. Riedel, Phys. Rev. B **25**, 264 (1982).

<sup>10</sup>G. Jug, Phys. Rev. B **27**, 609 (1983).

<sup>11</sup>I. O. Mayer, J. Phys. A **22**, 2815 (1989).

<sup>12</sup>J. C. Le Guillou and J. Zinn-Justin, Phys. Rev. B **21**, 3976 (1980).

<sup>13</sup>D. P. Landau, Phys. Rev. B **22**, 2450 (1980).

<sup>14</sup>J. Marro, A. Labarta, and J. Tejada, Phys. Rev. B **34**, 347 (1986); D. Chowdhury and D. Stauffer, J. Stat. Phys. **44**, 203 (1986); P. Braun and M. Föhnle, *ibid.* **52**, 775 (1988); P. Braun *et al.*, Int. J. Mod. Phys. B **3**, 1343 (1989).

<sup>15</sup>J. S. Wang and D. Chowdhury, J. Phys. (Paris) **50**, 2905 (1989).

<sup>16</sup>T. Holey and M. Föhnle, Phys. Rev. B **41**, 11 709 (1990).

<sup>17</sup>M. Hennecke, Phys. Rev. B **48**, 6271 (1993).

<sup>18</sup>H. O. Heuer, J. Phys. A **26**, L333 (1993).

<sup>19</sup>S. Wiseman and E. Domany, cond-mat/9802095 (unpublished); cond-mat/9802102 (unpublished).

<sup>20</sup>D. Stauffer and A. Aharony, *Introduction to the Percolation Theory* (Taylor & Francis, London, 1994).

<sup>21</sup>H. G. Ballesteros, L. A. Fernández, V. Martín-Mayor, A. Muñoz Sudupe, G. Parisi, and J. J. Ruiz-Lorenzo, Phys. Lett. B **400**, 346 (1997).

<sup>22</sup>A. Aharony and A. B. Harris, Phys. Rev. Lett. **77**, 3700 (1996).

<sup>23</sup>P. H. Barrett, Phys. Rev. B **34**, 3513 (1986).

<sup>24</sup>R. J. Birgeneau *et al.*, Phys. Rev. B **27**, 6747 (1983).

<sup>25</sup>N. Rosov, A. Kleinhammes, P. Lidbjörk, C. Hohenemser, and M. Eibschütz, Phys. Rev. B **37**, 3265 (1988).

<sup>26</sup>J. M. Hastings, L. M. Corliss, and W. Kunmann, Phys. Rev. B **31**, 2902 (1985).

<sup>27</sup>T. R. Thurston, C. J. Peters, R. J. Birgeneau, and P. M. Horn, Phys. Rev. B **37**, 9559 (1988).

<sup>28</sup>P. W. Mitchell *et al.*, Phys. Rev. B **34**, 4719 (1986).

<sup>29</sup>D. P. Belanger, A. R. King, and V. Jaccarino, Phys. Rev. B **34**, 452 (1986).

<sup>30</sup>M. Falcioni, E. Marinari, M. L. Paciello, G. Parisi, and B. Taglienti, Phys. Lett. **108B**, 331 (1982); A. M. Ferrenberg and R. H. Swendsen, Phys. Rev. Lett. **61**, 2635 (1988).

<sup>31</sup>F. Cooper, B. Freedman, and D. Preston, Nucl. Phys. B **210**, 210 (1989).

<sup>32</sup>H. G. Ballesteros, L. A. Fernández, V. Martín-Mayor, and A. Muñoz Sudupe, Phys. Lett. B **378**, 207 (1996); **387**, 125 (1996); Nucl. Phys. B **483**, 707 (1997).

<sup>33</sup>U. Wolff, Phys. Rev. Lett. **62**, 361 (1989).

<sup>34</sup>R. H. Swendsen and J. S. Wang, Phys. Rev. Lett. **58**, 86 (1987).

<sup>35</sup>M. N. Barber, in *Phase Transitions and Critical phenomena*, edited by C. Domb and J. L. Lebowitz (Academic, New York, 1983), Vol. 8.

<sup>36</sup>H. G. Ballesteros *et al.*, cond-mat/9805125 (unpublished).

<sup>37</sup>K. Binder, Z. Phys. B **43**, 119 (1981).